IOPscience iopscience.iop.org

Home Search Collections Journals About Contact us My IOPscience

Evidence of the lattice site change of Hf impurity from Hf-doped to Hf:Mg-codoped $LiNbO_3$ single crystals by extended X-ray absorption fine-structure spectroscopy

This article has been downloaded from IOPscience. Please scroll down to see the full text article.

1994 J. Phys.: Condens. Matter 6 L677

(http://iopscience.iop.org/0953-8984/6/44/006)

View the table of contents for this issue, or go to the journal homepage for more

Download details:
IP Address: 171.66.16.151
The article was downloaded on 12/05/2010 at 20:57

Please note that terms and conditions apply.

J. Phys.: Condens. Matter 6 (1994) L677–L680. Printed in the UK

LETTER TO THE EDITOR

Evidence of the lattice site change of Hf impurity from Hf-doped to Hf:Mg-codoped $LiNbO_3$ single crystals by extended x-ray absorption fine-structure spectroscopy

C Prieto and C Zaldo

Instituto de Ciencia de Materiales de Madrid, Consejo Superior de Investigaciones Científicas, Cantoblanco, Ciencias (C-4), E-28049 Madrid, Spain

Received 11 August 1994

Abstract. Extended x-ray absorption fine structure (EXAFS) spectroscopy has been applied to the study of the local environment of Hf in $LiNbO_3$ single crystals and to the influence of codoping with $\simeq 6\%$ of Mg on the site impurity. The change in the obtained radial distribution function shows the different environment for Hf in Hf:$LiNbO_3$ and Hf:Mg:$LiNbO_3$ samples which is related to the different site occupied in the matrix by the Hf ions. It has been found that the mean distance from the Hf to the first oxygen shell is larger in the samples codoped with Mg than in single-doped samples.

$LiNbO_3$ is a relevant material because of its application to optoelectronics technology as photorefractive devices [1] and solid state laser matrices [2]. In those applications, foreign ions in the materials play a major role because they are responsible for the modification of the optical properties. The optical work performed recently [3] is related to the laser performance of rare earth ions inside $LiNbO_3$. The optical properties of these potential laser materials are related to the lattice position of impurities. The impurity location is similar for other impurities, and it can be studied in transition metals in order to understand the problem. The addition of Mg as a second impurity to $LiNbO_3$ is responsible for the photorefractive response inhibition [4] and for the optical damage threshold enhancement [5].

In the single-doped crystal, Hf has been determined to be located at the Li site by EXAFS [6] and channelling [7] techniques. A recent work shows that the lattice site occupation of Hf in $LiNbO_3$ has a gradual transfer from the Li to the Nb site on increasing the Mg content [8]. The studied range, from 0 to 6% for the Mg-codoping concentration, results in complete transferral of Hf from one site to the other. EXAFS spectroscopy provides direct information on the nature, number and distance of the neighbours of the atom tested. From this information the lattice site location of the impurity may be inferred and the impurity environment can be determined [6, 9].

In this work we compare the environment information obtained from the EXAFS spectroscopy of Hf ions in Hf:$LiNbO_3$ and Hf:Mg(6%)$LiNbO_3$ crystals. In addition, it is shown that the distance from the impurity to the first oxygen neighbours is larger in samples codoped with Mg than in single-doped samples.

The $LiNbO_3$ structure has been determined by neutron and x-ray diffraction [10]. The structure is made up of shared-face irregular oxygen octahedra piled along the ferroelectric c axis. The octahedra are occupied by cations in the sequence Li, Nb and a vacancy octahedron. Furthermore, both Li and Nb are displaced (in opposite directions) along the c

0953-8984/94/440677+04$19.50 © 1994 IOP Publishing Ltd

axis towards the neighbouring vacancies: in this way there are two different distances from the cation to the oxygen neighbours.

$LiNbO_3$ single crystals with congruent Li/Nb melting ratio were grown by the Czochralski method. The molar impurity concentrations in the melt were Hf(1%):$LiNbO_3$ and Hf(1%):Mg(6%):$LiNbO_3$. Samples were plates, cut with their large faces perpendicular to the c axis. This axis was placed in the horizontal plane of the machine and tilted at about 45° with respect to the x-ray beam. Bragg diffractions were avoided by spatially shielding the detector window. Fluorescence spectra were acquired at room temperature at the Hf L_{III} absorption edge. We used synchrotron radiation emitted by the DCI storage ring of the Laboratoire pour l'Utilization du Rayonnement Electromagnetique (Orsay), running at 1.85 GeV with an average current of 250 mA. X-rays were monochromatized using a Si (311) two-crystal spectrometer. The energy calibration was monitored using a Cu foil sample, and was set as 8991 eV at the first maximum above the edge. The incident beam intensity was measured by an ion chamber, and detection of the total x-ray fluorescence was carried out using a plastic scintillator attached to a photomultiplier [11].

Figure 1 shows the EXAFS spectrum of Hf contained in the Hf:Mg:$LiNbO_3$ sample. A classical procedure has been used to analyse the spectra: to obtain the EXAFS signal, $\chi(E)$, the background of the measurement has been removed by a cubic spline fitting polynomial [12]. The analysis of the EXAFS signal to get the position of the neighbours around the impurity has been carried out using the well known EXAFS expression [13]:

$$\chi(k) = \sum_j \frac{N_j}{kR_j^2} \exp(-2k^2\sigma_j^2) \exp(-\Gamma_j R_j/k) f_j(k) \sin[2kR_j + \Phi_j(k)]. \quad (1)$$

This expression describes the EXAFS oscillations for a Gaussian distribution of neighbours around the central atom, in the single-scattering theory and in the plane-wave approximation. k is the wavevector of the photoelectron, which is related to the electron mass (m_e) and the threshold energy (E_0) by $k = [2m_e(E - E_0)/\hbar^2]^{1/2}$. N_j is the average coordination number for the Gaussian distribution of distances centred at the R_j value, σ_j is the Debye–Waller contribution, $\phi_j(k) = 2\delta(k) + \gamma_j(k)$ is the phase shift, $\delta(k)$ and $\gamma_j(k)$ being the central and backscattering atom phase shifts respectively, $f_j(k)$ is the amplitude of the backscattering atoms and Γ_j is related to the mean free path of the photoelectron.

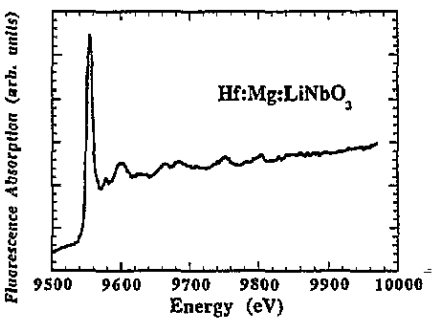

Figure 1. Room-temperature fluorescence EXAFS Hf spectra of Hf:Mg-codoped $LiNbO_3$ single crystal.

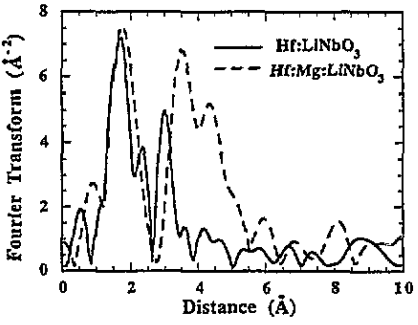

Figure 2. Fourier transform magnitude of the $k\chi(k)$ function for Hf:$LiNbO_3$ (solid line) and Hf:Mg:$LiNbO_3$ samples (broken line). The Hanning window of the transformation is from $k = 3.7$ to 10.20 Å^{-1}.

Figure 2 shows the modulus of the Fourier transform of the $k\chi(k)$ function (hereafter we refer to this function as pRDF) obtained for the single-doped sample (EXAFS data have been

reported previously [6]) and for the codoped one. In order to allow comparison between those samples doped with Mg and those that are not, the k range of the $k\chi(k)$ function selected to perform the Fourier transform has been kept constant. In both cases, a first significant peak appears at an apparent distance lower than $\simeq$ 2.0 Å. This peak is due to the six oxygens forming the first coordination shell. In the Hf:Mg:$LiNbO_3$ sample, it seems to be displaced to higher distances. As in previous EXAFS studies on the lattice site of impurities in $LiNbO_3$ [9], it can be shown that the peaks of the pRDF function appearing at distances larger than 2.0 Å are mainly related to the niobium ions of the lattice. The contribution of oxygen shells other than the first one has usually been found to be minor compared with that corresponding to niobiums. The possible contribution of Li ions has been ignored because of their very low electron backscattering amplitude.

It can be observed in figure 2 that the Fourier transform magnitude is completely different in the single-doped and the Mg-codoped samples, which denotes a change in the environment of the impurity. In order to determine the actual position of the Hf impurity, a quantitative analysis must be performed.

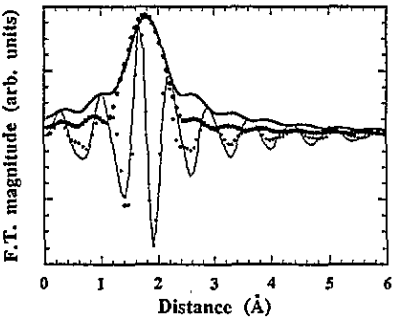

Figure 3. Distance-space comparison between calculated pRDF (solid line) and experimental filtered data (discrete points) of the modulus and imaginary part of the Fourier transform for the oxygen coordination of Hf in Hf:Mg:$LiNbO_3$ codoped sample.

Table 1. EXAFS parameters obtained as the best fit to equation (1). The number of neighbours has been fixed to the total coordination given by the crystallographic data.

Sample	Pair	N_j	R_j (Å)	σ (Å)	ΔE_0 (eV)
Hf:$LiNbO_3$	Hf–O	6	2.03 ± 0.03	0.09	−10.0
	Hf–Nb	1	2.69 ± 0.04	0.07	−12.0
	Hf–Nb	6	3.24 ± 0.04	0.07	−12.0
Hf:Mg:$LiNbO_3$	Hf–O	6	2.20 ± 0.03	0.07	−20.0
	Hf–Nb	6	3.70 ± 0.04	0.06	− 6.0

Table 1 shows the EXAFS parameters fitted with equation (1) for the different coordination spheres of the impurity. Fits have been performed using the calculated backscattering functions reported by Rehr *et al* [14]. Figure 3 shows the fit of the Fourier transform modulus and imaginary part for the first peak of the pRDF of Hf:Mg:$LiNbO_3$. All fits have been performed over a range larger than 1 Å and 6 $Å^{-1}$ in the R- and k-spaces respectively, in order to ensure a number of independent parameters better than four. In our case, only three free EXAFS parameters have been fitted because the coordination is fixed by the crystalline matrix. It can be noted that the obtained values of the threshold energy shifts are different from one sample to the other, and this opens the possibility of a different oxidation state on Hf, but it is not responsible for the different Hf–O distances in the two samples.

By looking at the Hf–Nb distances obtained for the Hf:Mg:$LiNbO_3$ sample, it is easy to identify the six Nb neighbours as analogous to the six Nb–Nb distances corresponding to the a and b lattice parameters ($a = b = 3.765$ Å). Those are the first Nb–Nb distances present in the lattice (the next ones are more than 5 Å). If one looks for Li–Nb distances to compare with the obtained Hf–Nb ones, the crystallographic data are 3.01, 3.05, 3.38 and 3.92 Å (the coordination numbers are 1, 3, 3 and 1, respectively). It is not possible to explain the EXAFS results with the Li-site position for Hf in the Hf:Mg:$LiNbO_3$ sample. On the other hand, in the single-doped Hf:$LiNbO_3$ it is possible to allow displacement of the Hf ions along the c axis to the centres of the octahedra so they are closer to the first Nb neighbour and to have a mean distance to the six next neighbours. In that way, the EXAFS data agree with the transferral from the Li- to the Nb-site position when 6% of Mg is present in $LiNbO_3$, as was proposed after channelling experiments [8].

The larger Hf–O distance obtained for the codoped sample can be explained as follows, even taking into account that the oxygen octahedra containing the Nb are smaller than those containing the Li atoms. The reason for the larger impurity–oxygen distance when the samples are also Mg doped must be that the Mg^{2+} ions are near the impurities. As the Mg^{2+} is supposed to be placed in the Li-lattice site there is a local increase of charge, and the Mg octahedra must be smaller than their similar Li octahedra; this gives the possibility of a softness of the surroundings and the nearest octahedra can be bigger. Moreover, the Mg^{2+}–Hf^{4+} gives the same charge as the Li^{+}–Nb^{5+} lattice pair, and the mean potential will not turn out very distorted. A similar case is that for impurities with an oxidation state of 5+; Ta:$LiNbO_3$ has been probed, and the Ta^{5+} are located at the Nb octahedra [6], where there is no electric charge distortion in the lattice.

We have shown by EXAFS spectroscopy that the position of the Hf impurity in $LiNbO_3$ changes from the Li site to the Nb one when the sample is codoped with 6% of Mg. The distance from the impurity to the oxygen neighbours turns out to be larger in the codoped sample, and this can be related to the proximity of the Mg impurity. This fact could be the basis of the explanation of the photorefractive effect inhibition and of the optical damage threshold enhancement by Mg codoping of the samples.

The authors wish to acknowledge the experimental facilities given by LURE (Orsay, France).

References

[1] Kratzig E and Schrimer O F 1988 *Photorefractive Materials and their Applications I (Topics in Applied Physics 61)* ed P Gunter and J P Huignard (Berlin: Springer) ch 5
[2] Fan T Y, Cordova-Plaza A, Digonnet M J F, Byer R L and Shaw H J 1986 *J. Opt. Soc. Am.* B **3** 140
[3] Tocho J O, Sanz-García J A, Jaque F and García-Solé J 1991 *J. Appl. Phys.* **70** 5582
[4] Volk T R, Pryalkin V I and Rubinina N M 1994 *Opt. Lett.* **15** 996
[5] Brian D A, Gerson R and Tomaschke H E 1984 *Appl. Phys. Lett.* **44** 847
[6] Prieto C, Zaldo C, Fessler P, Dexpert H, Sanz-García J A and Diéguez E 1991 *Phys. Rev.* B **43** 2594
[7] Rebouta L, Soares J C, da Silva M F, Sanz-García J A, Dieguez E and Agullo-Lopez F 1992 *J. Mater. Res.* **7** 130
[8] Rebouta L, da Silva M F, Soares J C, Santos M T, Dieguez E and Agullo-Lopez F 1994 *Radiat. Eff. Defects Solids* at press
[9] Zaldo C, Prieto C, Dexpert H and Fessler P 1991 *J. Phys.: Condens. Matter* **3** 4135
[10] Abrahams S C, Reddy J M and Bernstein J L 1966 *J. Phys. Chem. Solids* **27** 997
[11] Tourillon G, Guay D, Lemmonier M, Bortol F and Badeyan M 1990 *Nucl. Instrum. Methods* A **294** 382
[12] Bonnin D, Kaiser P and Desbarres J 1992 *EXAFS PC-software, 8th Europhysics School in Chemical Physics (La Rabida, 1992)*
[13] Koningsberger D C and Prins R 1988 *X-ray Absorption Principles, Applications, Techniques of EXAFS, SEXAFS and XANES* (New York: Wiley)
[14] Rehr J J, Mustre de Leon J, Zakinsky S I and Albers R C 1991 *J. Am. Chem. Soc.* **113** 5135